Tomographic velocity analysis of PP- and PS-waves for VTI media: Field-data application

Pengfei Cai[1,2] & Ilya Tsvankin[1]

[1] *Center for Wave Phenomena, Colorado School of Mines, Golden, CO, USA*
[2] *CGG, 10300 Town Park Dr, Houston, TX, USA*

ABSTRACT

Mode-converted PS-waves can provide valuable information for anisotropic parameter estimation that cannot be obtained from compressional waves alone. In a previous paper, we developed an efficient tomographic methodology for 2D joint velocity analysis of PP and PS data from VTI (transversely isotropic with a vertical symmetry axis) media. The algorithm is designed to flatten image gathers of PP-waves as well as of pure SS reflections computed using the PP+PS=SS method. An important additional constraint is provided by codepthing of the migrated PP and SS sections. The model is divided into square cells, and the parameters V_{P0}, V_{S0}, ϵ, and δ are defined at each grid point. Here, this methodology is applied to multicomponent data recorded on a 2D line from an OBS (ocean bottom seismic) survey acquired at Volve field in the North Sea. Although the parameter-updating procedure did not include any borehole information, the VTI model obtained by joint tomography of the recorded PP-waves and constructed SS-waves produced generally well-focused PP and PS depth images. The depth consistency between the migrated PP and PS sections also corroborates the accuracy of the velocity-analysis algorithm.

Key words: velocity analysis, PS-waves, VTI, codepthing, OBS data

1 INTRODUCTION

Multicomponent data can improve reservoir imaging and provide useful information for lithology, fluid, and fracture characterization. For example, shear waves help in imaging of reservoirs beneath gas clouds, where P-waves suffer from high attenuation (Tsvankin, 2005).

PS-waves are usually more sensitive to anisotropy than P-waves and can be used to constrain not just the vertical shear-wave velocity but also the subset of the medium parameters responsible for P- and S-wave propagation. In particular, combining PP and PSV reflections in VTI media may help estimate all four pertinent Thomsen parameters – the P- and S-wave vertical velocities (V_{P0} and V_{S0}) and the anisotropy coefficients ϵ and δ (Tsvankin and Grechka, 2011).

Joint tomographic inversion of PP and PS data has been discussed in several publications (Stopin and Ehinger, 2001; Audebert et al., 1999; Broto et al., 2003; Foss et al., 2005). However, velocity analysis of mode convertions is hampered by the asymmetry of PS moveout (i.e., PS traveltimes generally do not stay the same when the source and receiver are interchanged) and polarity reversals of PS-waves.

The methodology proposed in our previous publication (Cai and Tsvankin, 2012) overcomes the problems caused by the moveout asymmetry of PS-waves and takes advantage of efficient MVA (migration velocity analysis) algorithms designed for pure modes. Instead of using PS-waves directly for parameter estimation, we employ the PP+PS=SS method of Grechka and Tsvankin (2002) to generate the traveltimes of the corresponding pure SS reflections, which have symmmetric moveout. Then the computed SS-waves are combined with the recorded PP-waves to build a 2D VTI velocity model. Our algorithm for updating the parameters V_{P0}, V_{S0}, ϵ, and δ is based on the gridded reflection tomography developed for P-waves by Wang and Tsvankin (2013). In addition to removing residual moveout in image gathers, the algorithm penalizes depth misties between the migrated PP and SS sections and regularizes the solution using a finite-difference approximation of the Laplacian operator.

Here, the methodology of Cai and Tsvankin (2012) is applied to OBS data from Volve field in the North Sea (courtesy of Statoil). We start by briefly describing the algorithm for joint tomographic inversion of PP and PS data, the geological setting of the field, and the acqusition parameters of the survey. Registration of the PP- and PS-waves on a 2D line from the survey produces five events used for computing the

traveltimes of the pure SS-waves. The VTI velocity model for the line is obtained by tomographic velocity analysis of the PP and SS data that includes codepthing of the five picked reflectors on the migrated PP and SS sections. Finally, the images of the recorded PP- and PS-waves are compared to those computed with the velocity model previously obtained by Statoil.

2 METHODOLOGY

The algorithm of Cai and Tsvankin (2012) operates with 2D PP and PS reflection data. The first processing step is event registration (correlation) followed by application of the PP+PS=SS method to construct the pure SS reflections with the correct kinematics. The velocity model is built by extending the P-wave MVA algorithm of Wang and Tsvankin (2013) to multicomponent (PP and SS) data. The parameters V_{P0}, V_{S0}, ϵ, and δ are defined on a grid by dividing the section into square cells. For purposes of migration velocity analysis, we apply prestack Kirchhoff depth migration to the recorded PP and constructed SS data. The initial model may be obtained from stacking-velocity tomography at borehole locations (Wang and Tsvankin, 2010) or nonhyperbolic moveout analysis (as done in the case study below).

The objective function used in the joint MVA of PP- and SS-waves is defined as follows:

$$\begin{aligned} F(\Delta\boldsymbol{\lambda}) &= \mu_1||\mathbf{A}_P\,\Delta\boldsymbol{\lambda}+\mathbf{b}_P||^2+\mu_2||\mathbf{A}_S\,\Delta\boldsymbol{\lambda}+\mathbf{b}_S||^2 \\ &+ \mu_3||\mathbf{D}\,\Delta\boldsymbol{\lambda}+\mathbf{y}||^2+\zeta||L\,\Delta\boldsymbol{\lambda}||^2, \end{aligned} \tag{1}$$

where $\Delta\boldsymbol{\lambda}$ is the update of the vector $\boldsymbol{\lambda}$ of medium parameters, the matrices $\mathbf{A}_P$ and $\mathbf{A}_S$ include the derivatives of the PP and SS migrated depths with respect to the elements of $\boldsymbol{\lambda}$ (medium parameters), the vectors $\mathbf{b}_P$ and $\mathbf{b}_S$ characterize the residual moveout in PP- and SS-wave CIGs, the matrix $\mathbf{D}$ describes the differences between the derivatives of the PP and SS migrated depths with respect to the medium parameters, and the vector $\mathbf{y}$ contains the differences between the migrated depths on the PP and SS sections. Flattening PP and SS common-image gathers (CIGs) minimizes the first two terms ($||\mathbf{A}_P\Delta\boldsymbol{\lambda}+\mathbf{b}_P||^2$ and $||\mathbf{A}_S\Delta\boldsymbol{\lambda}+\mathbf{b}_S||^2$), and codepthing is achieved through minimizing the third term ($||\mathbf{D}\Delta\boldsymbol{\lambda}+\mathbf{y}||^2$). The regularization term ($||L\Delta\boldsymbol{\lambda}||$) helps stabilize the inversion. The coefficients μ_1, μ_2, μ_3 and ζ determine the weights of the corresponding terms.

The objective function is minimized by a least-squares algorithm. Since the VTI parameters are updated at each grid point, which makes the inversion time-consuming, we parallelize our algorithm. Common-image gathers for each reflector are computed on different cores, and flattening of PP and SS events is performed simultaneously.

3 APPLICATION TO FIELD DATA

3.1 Description of Volve field and OBS survey

Volve field is a Middle Jurassic oil reservoir located in the southern part of the Viking Graben in the gas/condensate-rich Sleipner area of the North Sea. It is a small dome-shaped structure formed by the collapse of adjacent salt ridges during the Jurassic (Szydlik et al., 2007). The reservoir is in the Middle Jurassic Hugin Sandstone Formation and the deposition was controlled by salt tectonics.

An ocean-bottom seismic (OBS) survey at Volve field was acquired in 2002 over a 12.3 km $\times$ 6.8 km area. It is comprised of six swaths of four-component (4C) data and each swath includes two 6 km-long cables placed on the seafloor. The cables have a 400 m spacing and move up 800 m after each swath. There are 240 receivers with an interval of 25 m on each cable. Dual-source flip-flop shooting gave a 25 m shot separation and 100 m separation between sail lines.

The PP and PS OBS data were preprocessed using a standard sequence including wavelet shaping, noise and multiple attenuation techniques (Szydlik et al., 2007). The VTI model produced by Statoil for prestack depth imaging is built using a layer-stripping approach. Each layer is updated by applying layer-based tomography and fitting check-shot data (Szydlik et al., 2007). The algorithm involves iterative flattening of common-image gathers and minimization of the misties between seismic and well data. However, complete information about the VTI model-building process employed by Statoil is unavailable to us.

3.2 Processing/inversion of PP and PS data

We use a 2D section from the 3D PP- and PS-wave data recorded by the cable laid along $y=2.8$ km. PP-waves from the same line were processed by Wang (2012), who built a TTI model using reflection tomography. Two adjacent source lines ($y=2.8\pm0.025$ km) include 481 shots with a shot interval of 25 m.

The joint MVA of PP- and PS-waves described above is applied to the CIGs from $x=3$ km to 9 km with an interval of 100 m. The initial model for the parameters V_{P0}, ϵ, and δ is taken from Wang (2012), who divided the section into eight layers based on key geologic horizons and applied nonhyperbolic moveout analysis in combination with check shots in two nearby wells. Since check-shot data for shear waves were not available, a smoothed version of the shear-wave vertical-velocity model provided by Statoil is used here as the initial V_{S0}-field. The parameters V_{P0}, V_{S0}, ϵ, and δ are defined on a 100 m $\times$ 50 m grid (Figure 1).

The PP and PS images migrated with the initial model are shown in Figure 2. There is a clearly visible mistie between the PP and PS sections for a reflector at a depth close to 2.5 km (top of the Cretaceous Unit); the depth of that reflector is smaller on the PS image. As expected, the CIGs of PP- and SS-waves obtained with the initial model parameters exhibit substantial residual moveout.

To apply the PP+PS=SS method, we registered (correlated) five events on the PP and PS stacked sections. For each of these five events pure shear data were constructed by convolving the computed SS traveltimes with a Ricker wavelet. The codepthing term in the objective function (equation 1) in-

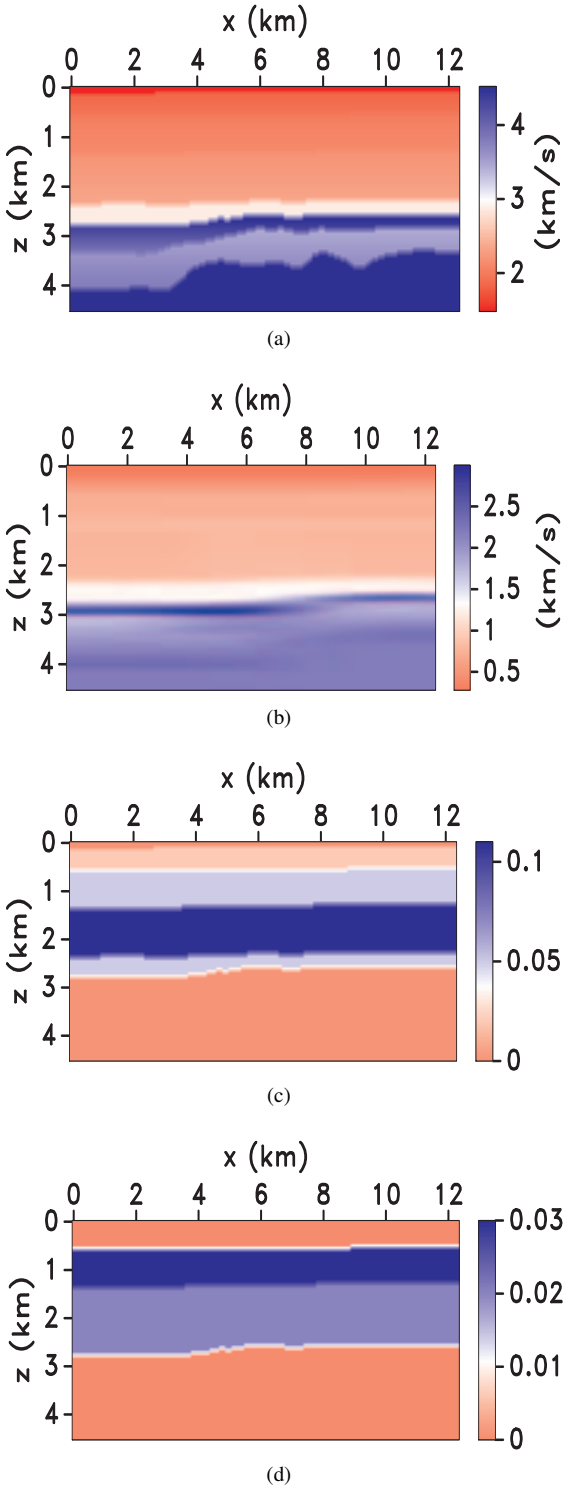

Figure 1. Initial VTI model for line y=2.8 km from the Volve survey. The vertical velocities (a) V_{P0} and (b) V_{S0} and the anisotropy parameters (c) ϵ and (d) δ.

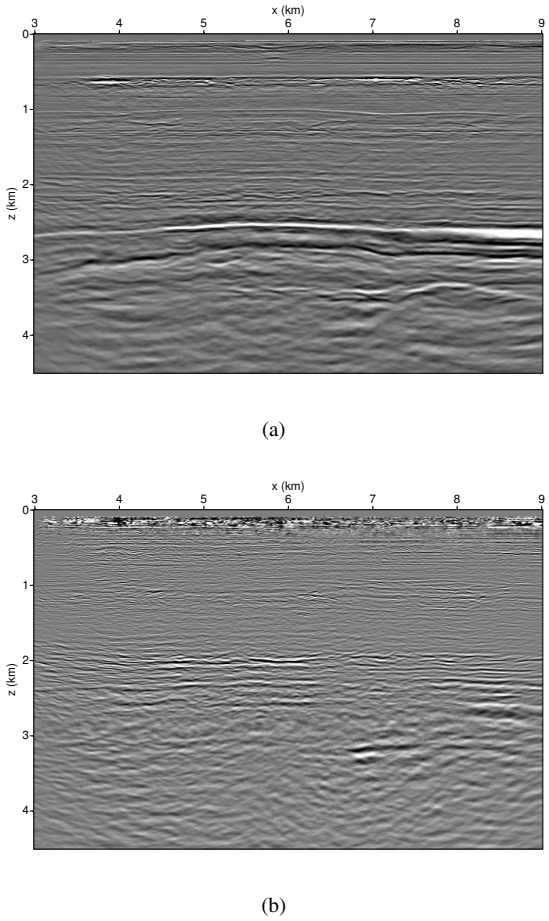

Figure 2. (a) PP- and (b) PS-wave images generated by Kirchhoff prestack depth migration with the initial model from Figure 1.

cludes the depths of these five reflectors on the PP and SS sections.

Because of the limited offset-to-depth ratio (smaller than 1.2 for z >3 km), the accuracy of the effective parameters η and ϵ estimated from nonhyperbolic moveout (i.e., long-spread CIGs) decreases with depth. Therefore, the deeper part of the section (z > 3 km) is kept isotropic during model updating. The VTI model obtained after eight iterations of joint MVA of PP- and PS-waves (Figure 3) yields relatively flat PP and SS CIGs and depth-consistent PP and SS images.

3.3 Images obtained with the inverted VTI model

The PS-wave depth image generated with the estimated VTI model is displayed in Figure 4. Compared with the section obtained using the initial model (Figure 2(b)), reflectors on the final image are better focused, especially at depths around 3 km (Cretaceous unit). However, the image quality below the Base Cretaceous unconformity is still lower than that for PP-waves (Figure 4(a)). This is probably because the deeper layers were

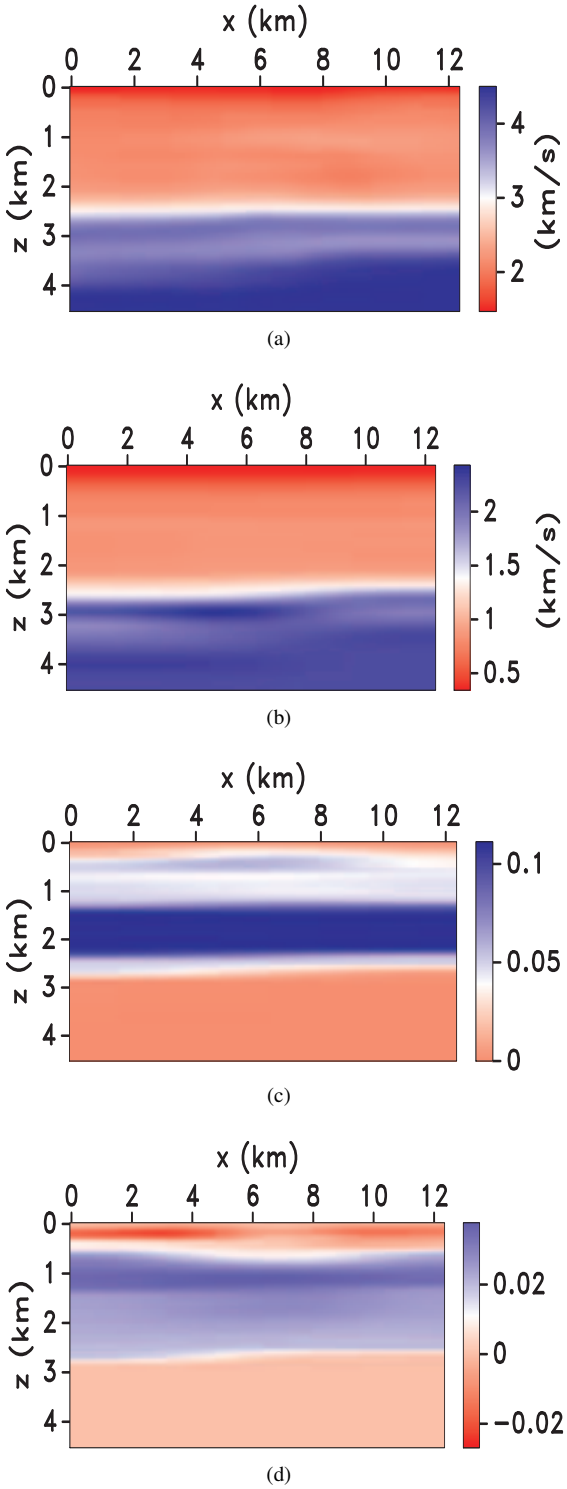

Figure 3. Estimated VTI model for line y=2.8 km from the Volve survey. The vertical velocities (a) V_{P0} and (b) V_{S0} and the anisotropy parameters (c) ϵ and (d) δ.

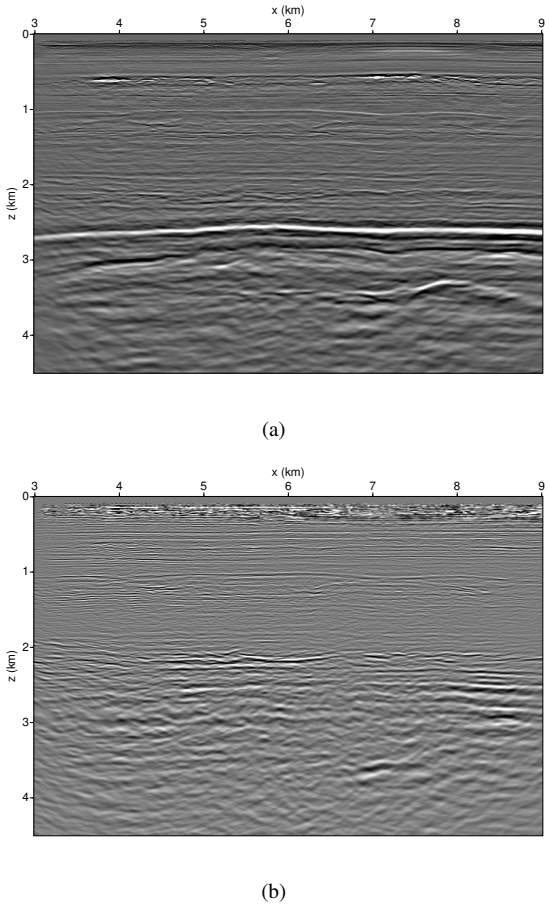

Figure 4. (a) PP- and (b) PS-wave depth images generated with the estimated model from Figure 3.

kept isotropic during MVA, and PS-waves are more sensitive to anisotropy than PP-waves.

The final PP image (Figure 4(a)) does not differ much from that obtained by Wang (2012) using P-wave tomography. However, the reflectors in the Cretaceous unit look somewhat less coherent than those imaged by Wang (2012). One possible reason is that we used a smaller number of reflectors in building the velocity model. Also, although the dips are gentle, the TTI model employed by Wang (2012) is more geologically plausible than VTI and may yield more accurate anisotropy parameters. It is likely that better PP and PS depth images can be obtained with a TTI model, but the current version of the algorithm does not allow for a tilt of the symmetry axis.

We were able to tie the PP depth image with the PS depth image down to Base Cretaceous unconformity (the deepest event used to generate SS data). These depth-consistent PP and PS images provide a robust estimate of the V_{P0}/V_{S0} ratio, which can be used for reservior characterization.

The final PP- and PS-wave images in Figure 4 are similar to those obtained with the VTI model provided by Statoil. It should be mentioned, however, that Statoil's parameter fields have a higher spatial resolution than the model in Figure

3 because our updating procedure operated only with reflection data. Clearly, there is still depth uncertainty in our images, which can be reduced by including borehole (e.g., VSP) information.

4 CONCLUSIONS

We carried out anisotropic processing of PP and PS data from Volve field in the North Sea using reflection tomography and Kirchhoff prestack depth migration. To avoid problems caused by the moveout asymmetry and other inherent features of mode conversions, PS-waves were replaced in velocity analysis with pure SS reflections generated by the PP+PS=SS method.

Registration (correlation) of the PP and PS sections helped identify five events that were used to compute the traveltimes of the corresponding SS-waves. Model updating was performed by flattening PP and SS image gathers and tying the five interfaces in depth on the migrated PP and SS images. The inverted sections of the parameters V_{P0}, V_{S0}, ϵ, and δ have a somewhat lower resolution than the corresponding sections obtained by Statoil with the help of borehole data. Nevertheless, the quality of the migrated images computed with our and Statoil's models is similar. The limited offset range of the survey did not allow us to estimate the anisotropy parameters below 3 km, which hampered the focusing of the deeper reflectors. It should be emphasized that the PP and PS sections are tied in depth down to the Base Cretaceous unconformity (the deepest event used to construct SS data).

Further improvement can be achieved by including walkaway VSP or other borehole data in the tomographic inversion and taking into account a possible tilt of the symmetry axis. On the whole, however, this case study demonstrates that combining PP-waves with mode conversions in anisotropic tomography results in depth-consistent PP and PS images, increases the accuracy of VTI velocity models, and provides estimates of the V_{P0}/V_{S0} ratio for lithology prediction and reservoir characterization.

5 ACKNOWLEDGMENTS

We would like to thank Statoil ASA and the Volve license partners ExxonMobil E&P Norway and Bayerngas Norge for the release of the Volve data. The viewpoints about the Volve data in this paper are of the authors and do not necessarily reflect the views of Statoil ASA and the Volve license partners. We also acknowledge the helpful suggestions of Marianne Houbiers of Statoil. We are grateful to our colleagues from the Center for Wave Phenomena (CWP) for valuable technical assistance. The support for this work was provided by the Consortium Project on Seismic Inverse Methods for Complex Structures at CWP.

REFERENCES

Audebert, F., P. Y. Granger, and A. Herrenschmidt, 1999, CCP-scan technique (1): True common conversion point sorting and converted wave velocity analysis solved by PP and PS Pre-Stack Depth Migration: SEG Technical Program Expanded Abstracts, **18**, 1186–1189.

Broto, K., A. Ehinger, J. H. Kommedal, and P. G. Folstad, 2003, Anisotropic traveltime tomography for depth consistent imaging of PP and PS data: The Leading Edge, 114–119.

Cai, P., and I. Tsvankin, 2012, Joint migration velocity analysis of PP- and PS- waves for VTI media: CWP Research Report (CWP-715).

Foss, S.-K., B. Ursin, and M. V. de Hoop, 2005, Depth-consistent reflection tomography using PP and PS seismic data: Geophysics, **70**, U51–U65.

Grechka, V., and I. Tsvankin, 2002, PP+PS=SS: Geophysics, **67**, 1961–1971.

Stopin, A., and A. Ehinger, 2001, Joint PP PS tomographic inversion of the Mahogany 2D 4-C OBC seismic data: SEG Technical Program Expanded Abstracts, **20**, 837–840.

Szydlik, T., P. Smith, S. Way, L. Aamodt, and C. Friedrich, 2007, 3d pp/ps prestack depth migration on the volve field: First Break, **25**, 43–47.

Tsvankin, I., 2005, Seismic signatures and analysis of reflection data in anisotropic media, 2nd ed.: Elsevier Science Publishing Company, Inc.

Tsvankin, I., and V. Grechka, 2011, Seismology of azimuthally anisotropic media and seismic fracture characterization: Society of Exploration Geophysicists.

Wang, X., 2012, Anisotropic velocity analysis of p-wave reflection and borehole data: PhD thesis, Colorado School of Mines.

Wang, X., and I. Tsvankin, 2010, Stacking-velocity inversion with borehole constraints for tilted TI media: Geophysics, **75**, D69–D77.

———, 2013, Ray-based gridded tomography for tilted transversely isotropic media: Geophysics, **78**, C11–C23.